Optofluidic waveguides for reconfigurable photonic systems

Aram J. Chung and David Erickson*

Sibley School of Mechanical and Aerospace Engineering, Cornell University, Ithaca, New York 14853, USA
**de54@cornell.edu*

Abstract: We report the development of two liquid waveguide based photonic elements for use in reconfigurable photonic systems. This work demonstrates the ability to couple light from a conventional optical fiber to an adaptable liquid-core/liquid-cladding waveguide and back again to an optical fiber(s) enabling us to take advantage of both liquid- and solid-state photonic modalities. We demonstrate and characterize the use of this fiber-in and fiber-out system as either an optical switch or signal attenuator. Microscale flow control enables the adaptive morphology and tunable position of the liquid waveguide yielding an attenuation range of 3.1-10.7 dB, operability over a broad bandwidth spanning the range of wavelengths from visible to telecommunication, and a 1x2 sub-second switching system with a cross-talk as low as 20 dB and maximum coupling efficiency of 3.87 dB.

OCIS codes: (060.0060) Fiber optics and optical communications; (130.3120) Integrated optics devices; (130.4815) Optical switching devices; (160.2290) Fiber materials; (230.7370) Waveguides.

References and links

1. D. B. Strukov, and K. K. Likharev, "CMOL FPGA: a reconfigurable architecture for hybrid digital circuits with two-terminal nanodevices," Nanotechnology **16**(6), 888–900 (2005).
2. L. Y. Lin, and E. L. Goldstein, "Opportunities and challenges for MEMS in lightwave communications," IEEE J. Sel. Top. Quantum Electron. **8**, 163–172 (2002).
3. S. E. Lyshevski, *MEMS and NEMS: Systems, Devices, and Structures* (CRC Press, 2002).
4. M. Gad-el-Hak, *MEMS: Design and Fabrication* (CRC Press, 2006).
5. M. Roussey, M. P. Bernal, N. Courjal, and F. I. Baida, "Experimental and theoretical characterization of a lithium niobate photonic crystal," Appl. Phys. Lett. **87**, 241101 (2005).
6. M. Roussey, M. P. Bernal, N. Courjal, D. Van Labeke, F. I. Baida, and R. Salut, "Electro-optic effect exaltation on lithium niobate photonic crystals due to slow photons," Appl. Phys. Lett. **89**, 241110 (2006).
7. M. Diwekar, V. Kamaev, J. Shi, and Z. V. Vardeny, "Optical and magneto-optical studies of two-dimensional metallodielectric photonic crystals on cobalt films," Appl. Phys. Lett. **84**, 3112–3114 (2004).
8. F. Verluise, V. Laude, Z. Cheng, C. Spielmann, and P. Tournois, "Amplitude and phase control of ultrashort pulses by use of an acousto-optic programmable dispersive filter: pulse compression and shaping," Opt. Lett. **25**(8), 575–577 (2000).
9. N. Courjal, S. Benchabane, J. Dahdah, G. Ulliac, Y. Gruson, and V. Laude, "Acousto-optically tunable lithium niobate photonic crystal," Appl. Phys. Lett. **96**, 131103 (2010).
10. E. Camargo, H. Chong, and R. De La Rue, "2D Photonic crystal thermo-optic switch based on AlGaAs/GaAs epitaxial structure," Opt. Express **12**(4), 588–592 (2004).
11. L. L. Gu, W. Jiang, X. N. Chen, L. Wang, and R. T. Chen, "High speed silicon photonic crystal waveguide modulator for low voltage operation," Appl. Phys. Lett. **90**, 071105 (2007).
12. D. Erickson, C. H. Yang, and D. Psaltis, "Optofluidics emerges from the laboratory," Photon. Spectra **42**, 74–78 (2008).
13. D. Psaltis, S. R. Quake, and C. Yang, "Developing optofluidic technology through the fusion of microfluidics and optics," Nature **442**(7101), 381–386 (2006).
14. C. Monat, P. Domachuk, and B. J. Eggleton, "Integrated optofluidics: A new river of light," Nat. Photonics **1**, 106–114 (2007).
15. D. Erickson, T. Rockwood, T. Emery, A. Scherer, and D. Psaltis, "Nanofluidic tuning of photonic crystal circuits," Opt. Lett. **31**(1), 59–61 (2006).

#143705 - $15.00 USD Received 10 Mar 2011; revised 6 Apr 2011; accepted 6 Apr 2011; published 18 Apr 2011

16. C. L. Smith, U. Bog, S. Tomljenovic-Hanic, M. W. Lee, D. K. Wu, L. O'Faolain, C. Monat, C. Grillet, T. F. Krauss, C. Karnutsch, R. C. McPhedran, and B. J. Eggleton, "Reconfigurable microfluidic photonic crystal slab cavities," Opt. Express **16**(20), 15887–15896 (2008).
17. U. Levy, K. Campbell, A. Groisman, S. Mookherjea, and Y. Fainman, "On-chip microfluidic tuning of an optical microring resonator," Appl. Phys. Lett. **88**, 111107 (2006).
18. J. C. Galas, J. Torres, M. Belotti, Q. Kou, and Y. Chen, "Microfluidic tunable dye laser with integrated mixer and ring resonator," Appl. Phys. Lett. **86**, 264101 (2005).
19. D. B. Wolfe, R. S. Conroy, P. Garstecki, B. T. Mayers, M. A. Fischbach, K. E. Paul, M. Prentiss, and G. M. Whitesides, "Dynamic control of liquid-core/liquid-cladding optical waveguides," Proc. Natl. Acad. Sci. U.S.A. **101**(34), 12434–12438 (2004).
20. J. M. Lim, S. H. Kim, J. H. Choi, and S. M. Yang, "Fluorescent liquid-core/air-cladding waveguides towards integrated optofluidic light sources," Lab Chip **8**(9), 1580–1585 (2008).
21. S. K. Tang, C. A. Stan, and G. M. Whitesides, "Dynamically reconfigurable liquid-core liquid-cladding lens in a microfluidic channel," Lab Chip **8**(3), 395–401 (2008).
22. X. Mao, J. R. Waldeisen, B. K. Juluri, and T. J. Huang, "Hydrodynamically tunable optofluidic cylindrical microlens," Lab Chip **7**(10), 1303–1308 (2007).
23. Z. Li, Z. Zhang, T. Emery, A. Scherer, and D. Psaltis, "Single mode optofluidic distributed feedback dye laser," Opt. Express **14**(2), 696–701 (2006).
24. W. Z. Song, and D. Psaltis, "Pneumatically tunable optofluidic dye laser," Appl. Phys. Lett. **96**, 081101 (2010).
25. E. E. Jung, A. J. Chung, and D. Erickson, "Analysis of liquid-to-solid coupling and other performance parameters for microfluidically reconfigurable photonic systems," Opt. Express **18**(11), 10973–10984 (2010).
26. Y. C. Seow, S. P. Lim, and H. P. Lee, "Tunable optofluidic switch via hydrodynamic control of laminar flow rate," Appl. Phys. Lett. **95**, 114105 (2009).
27. J. M. Lim, J. P. Urbanski, T. Thorsen, and S. M. Yang, "Pneumatic control of a liquid-core/liquid-cladding waveguide as the basis for an optofluidic switch," Appl. Phys. Lett. In press.
28. G. M. Whitesides, E. Ostuni, S. Takayama, X. Jiang, and D. E. Ingber, "Soft lithography in biology and biochemistry," Annu. Rev. Biomed. Eng. **3**(1), 335–373 (2001).
29. E. E. Jung, A. J. Chung, and D. Erickson, "Advancements in microfluidically reconfigurable photonics " in *European Optical Society Conference on Optofluidics* (2011).
30. J. G. Bayly, V. B. Kartha, and W. H. Stevens, "The absorption spectra of liquid phase H_2O, HDO and D_2O from 0.7μm to 10μm," Infrared Phys. **3**, 211–222 (1963).

1. Introduction

A reconfigurable system is one that can dynamically adapt its properties or function in response to an externally issued command or autonomously in response to changes in operational conditions. In electronics, the FPGA (Field Programmable Gate Array) [1] is the ubiquitous example of such a system in that it can provide "on-the-fly" reconfigurability by reprogramming the hierarchy of interconnections between different logic blocks. Despite the advantages, there are very few other microsystem based fields which have demonstrated technologies that exhibit anywhere near the level of reconfiguration possible through FPGAs.

A key factor for the development of an analogous high-performance reconfigurable photonic system would be the capability to dynamically control either (1) the physical layout or (2) the refractive indices of the optical components. Recent advancements in optical MEMS technology [2–4] has provided significant functionality and flexibility to the former of these techniques. With regards to the latter, traditional techniques for manipulating the refractive index through electro-optic [5, 6], magneto-optic [7], acousto-optic [8, 9], thermo-optic [10], and carrier injection [11] techniques are limited by the achievable $\Delta n/n$ (see Erickson *et al.* [12] for details and a tabulated comparison). The practical implication of a smaller $\Delta n/n$ is that either a longer interaction length is required (occupying more on-chip space) or resonant elements must be incorporated (reducing the bandwidth).

Recent developments in optofluidics [13, 14] have demonstrated how incorporating microfluidic elements into photonic systems can yield much higher $\Delta n/n$. For example, Erickson *et al.* [15], reported high refractive index modulation of the photonic crystal circuits using nanofluidics. The disadvantage of these approaches is that while broad tunability can be obtained, the base optical elements (*e.g.* photonic crystals [15, 16] and ring resonators [17, 18]) must be incorporated at the fabrication stage. Although a number of pure fluid state photonic elements, like waveguides [19, 20], microlenses [21, 22], and dye lasers [23, 24] have been demonstrated, they are not often used to directly physically reconfigure elements

#143705 - $15.00 USD Received 10 Mar 2011; revised 6 Apr 2011; accepted 6 Apr 2011; published 18 Apr 2011

within a solid-state photonic system. The advantage of using fluidics in comparison with the MEMS based reconfigurability approaches listed above is that the physical displacement of the optical elements can be much larger.

In this paper, we demonstrate the use of high performance liquid-core/liquid-cladding waveguides to achieve optical attenuation and 1x2 switching in a fiber-in and fiber-out system. Previously we reported a numerical study [25] on a hybrid system for coupling light between liquid- and solid-state waveguides, demonstrating the potential to achieve high coupling efficiencies using a fluid enveloping "end-fire" type technique. Here we implement this technique experimentally demonstrate coupling efficiencies as high as 48.98% (including all losses from the input fiber to the output detector). Recently, Seow *et al.* [26] and Lim *et al.* [27] also reported liquid-core based switching systems, with the latter demonstrating a high-speed 2x3 fiber-in and fiber-out switch. Here we demonstrate analogous switching but also introduce: the ability to perform controlled the attenuation, a single layer fabrication technique optimized for achieving low cross-talk (less than 20 dB), and characterize the system over the broader bandwidth including visible and telecommunication wavelengths. By integrating liquid- and solid-state photonic modalities on a single chip, we hope this hybrid system can become an element of a new type of photonic element for use in reconfigurable photonic and optical communication systems.

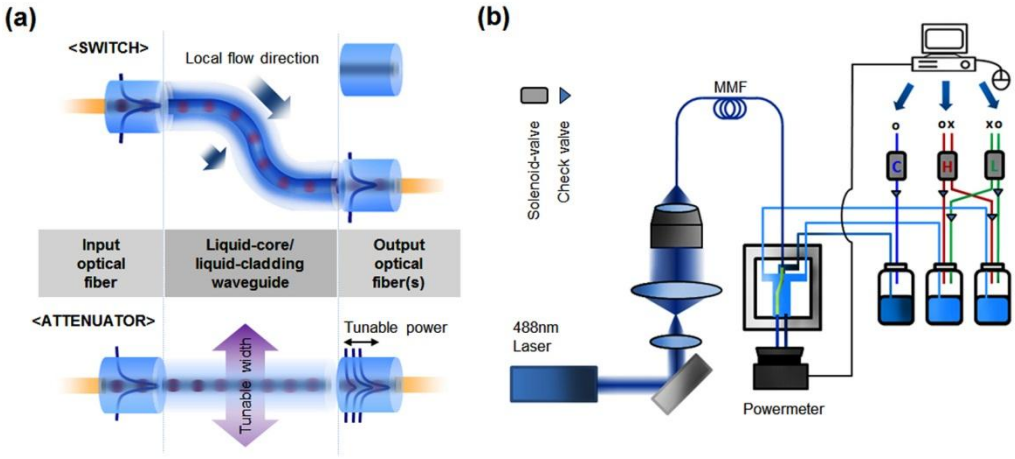

Fig. 1. Schematic views of (a) the optofluidic system showing the principle of operation for the optical switch (upper image) and the tunable modulator (lower image) (b) Experimental setup showing the coupling of the optical and flow control systems to the chip.

2. Principles of operation, device design and experimental setup

We demonstrate here two hybrid fiber-in and fiber-out reconfigurable optofluidic systems: (1) a 1x2 optical switch and (2) a tunable attenuator. The operating principle of both these devices is shown schematically in Fig. 1(a). Briefly, in both cases light is first coupled from the input optical fiber to the adaptable liquid-core/liquid-cladding waveguide. In the case of the switch the liquid waveguide is then directed to one of the two output fibers by changing the input pressure of one of the cladding flows. For the attenuator we modulate the power transferred from the input to the output optical fiber by adjusting the width of the liquid-core waveguide. This is done by increasing or decreasing the pressure of both cladding flows equally.

To form the liquid-core/liquid-cladding waveguide [19], a solution of 5.0 M Calcium Chloride ($CaCl_2$, n~1.44) is introduced as the core solution and two low refractive index streams of DI water (n~1.33) are used as the cladding. For the waveguide visualization experiments shown below, the core fluid was also doped with FITC (fluorescein

#143705 - $15.00 USD Received 10 Mar 2011; revised 6 Apr 2011; accepted 6 Apr 2011; published 18 Apr 2011

isothiocyanate) dye. For all excitation wavelengths multi-mode fiber (MMF, outer diameter = 125 μm, core diameter = 105 μm, and nominal numerical aperture NA = 0.22) was used for both the input and output channels. We used MMF here since they are often preferred to single mode fibers in optical communication due to their lower cost and relative ease of in-coupling. Unless otherwise noted below, all experiments were conducted with a 488 nm laser with the output power fixed at 4.3 mW. As illustrated in Fig. 1(b) the fiber is directly inserted into a poly(dimethylsiloxane)(PDMS) chip whose channel height was matched with that of the optical fiber outer diameter. The PDMS-microchannel was fabricated using a conventional soft photolithography method [28]. Flows are pumped into the PDMS microfluidic chip using off-chip solenoid-valves and all fluid flow manipulation which was controlled via a customized LabVIEW program as can be seen in Fig. 1(b).

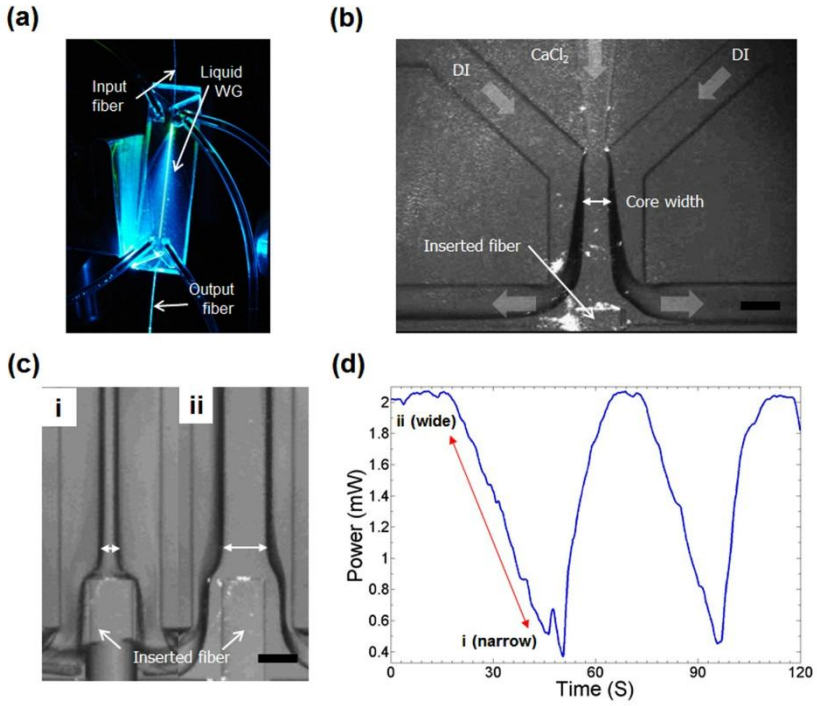

Fig. 2. Optofluidic tunable attenuator (a) PDMS chip showing liquid-core/liquid-cladding waveguide and light propagation along it. (b) Magnified view from above looking at the region near liquid waveguide. (c) Minimum and maximum transmitted power states for the liquid waveguide. (d) Output power measurements for the 1.25 mm liquid waveguide length: output (see supplemental Media 1). In all cases, scale bar represents 125 μm.

3. Results and discussion

3.1. Optofluidic attenuator

For the optofluidic attenuator, the input and output optical fibers are directly coupled by the liquid waveguide. By changing the width of the liquid core (by modulating the relative flow rates of the core and cladding fluids) the amount of power transmitted to the output fiber can be dynamically modulated. The mode profile in the liquid waveguide can be also reconfigured simply by adjusting the local flow conditions. Single mode operation is possible, as demonstrated by Wolfe *et al.* [19]. As mentioned above however, here we focus primarily on multimode operation. The optofluidically tunable attenuator and a magnified view of the microfluidic arrangement at the region near liquid waveguide are showed in Fig. 2(a) and 2(b) respectively. Figure 2(c) and 2(d) illustrate the transmitted power changes as the core is

#143705 - $15.00 USD Received 10 Mar 2011; revised 6 Apr 2011; accepted 6 Apr 2011; published 18 Apr 2011

adjusted from its maximum to minimum width (see supplemental Media 1 for more details). Based on the power output for the 1.25 mm waveguide length shown here, the observed attenuation power range was between 3.1 to 10.7 dB.

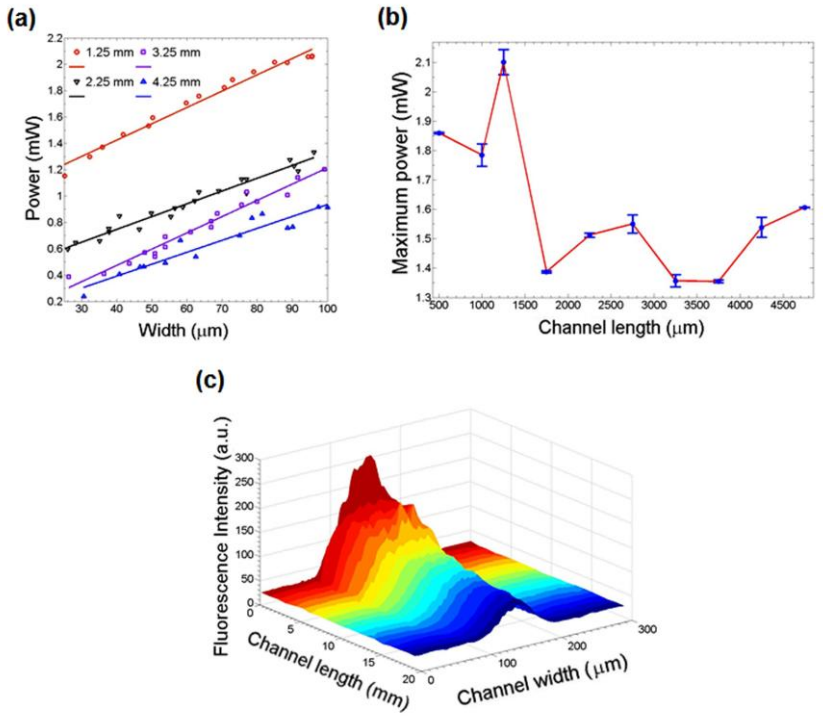

Fig. 3. (a) Output power as a function of the waveguide width for different channel lengths (equivalent to liquid waveguide length). (b) Maximum power as a function of the liquid waveguide length ranging from 0.5 mm to 4.75 mm. The error bars represents standard error of the mean. (c) Emitted fluorescence intensity from the liquid waveguide as a function of downstream distance.

In order to further characterize the optofluidic attenuator, a series of experiments were performed to measure the transmitted power as a function of the width and length of the liquid core waveguide. Figure 3(a) shows results for four different channel lengths: 1.25, 2.25, 3.25 and 4.25 mm. The method of least squares was used to fit the data points. Figure 3(b) shows the maximum transmitted power trend for all the waveguide lengths tested here. As can be seen in Fig. 3(a), regardless of the length of the liquid waveguide a linear response of the output power was observed as a function of the core width. It was however also observed that when the core size became much larger than that of the optical fiber, the transmitted power was also reduced. As expected, the maximum transmitted power tended to decrease for longer liquid waveguides. The inconsistency in the slope and variability in the maximum coupled power with waveguide length, seen in Figs. 3(a) and 3(b), was a repeatable effect and likely the result of irregular reflections off the waveguide surface and mode mismatching between the liquid waveguide and the output optical fiber. Commercially available tunable attenuators have a higher variable attenuation range but tend to have much higher power insertion loss. In addition, the material costs for manufacturing fluid based attenuators such as this one could be much lower, given that only 6 g of PDMS are required at an approximate cost of 50 cents.

To characterize the loss in the liquid waveguide itself we performed an experiment where the liquid waveguide was doped with a florescent dye and the change in emitted intensity was measured as a function of the downstream distance. Figure 3(c) shows the intensity profile for

#143705 - $15.00 USD Received 10 Mar 2011; revised 6 Apr 2011; accepted 6 Apr 2011; published 18 Apr 2011

a 120 μm wide waveguide for two centimeters of propagation distance. With these results, we calculate the waveguide loss is 0.451 dB/mm. Note that the waveguide loss calculated here includes the loss due to the florescent dye absorption. We expect that major cause for this loss was diffusive broadening of the core and cladding interface (see Jung *et al.* [25] for a numerical analysis of the relationship between light propagation and diffusion as a function of Peclet number). Reduction of this loss could be achieved through the use of immiscible fluids [29].

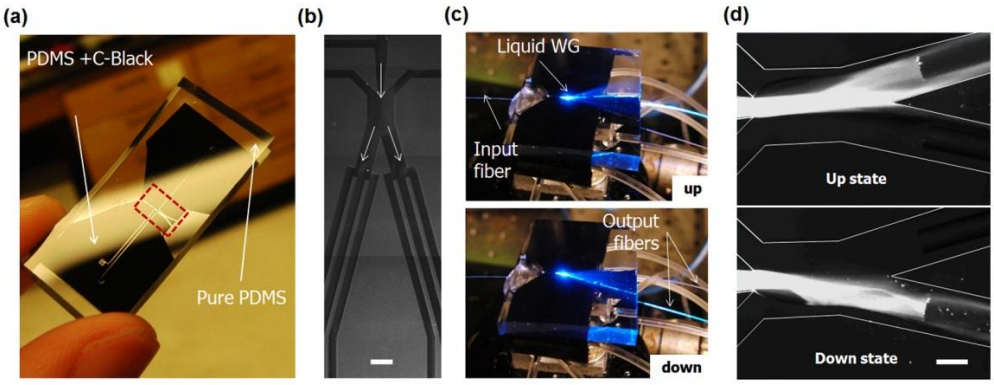

Fig. 4. (a) Optofluidic switch showing carbon black added to the bottom substrate in order to reduce cross-talk between the two output optical fibers. (b) Optical micrograph view of the red dashed zone in (a). (c) Photographic image of the 1x2 optofluidic switch in both states. (d) Magnified view of the switching states. (see supplemental Media 2). In all cases, scale bar represents 125 μm.

3.2. Optofluidic switch

As briefly mentioned above, the optofluidic switching element operates through pressure manipulation of the core and cladding fluids, directing the position of the liquid waveguide so that it out couples to one of the output optical fibers. Figure 4(a) shows the optofluidic chip and Fig. 4(b) shows a magnified view of the microfluidic channel layout. To reduce cross-talk between the two output channels, carbon black was introduced during the PDMS polymerization process (2.4% wt/wt with a 5:1 mass ratio of the base to the curing agent for the PDMA). Optofluidic switching between the two states of a 1x2 switch is shown in Figs. 4(c) and 4(d) (see supplemental Media 2 for more details). In both these figures the liquid waveguide was doped with fluorescent dye to facilitate visualization. Note that the presence of the carbon black significantly interferes with fluorescent imaging, resulting relative poor quality of the images. In this paper, we demonstrate a 1x2 switching system however we note that it could be expanded to a 1xN system for higher performance applications.

#143705 - $15.00 USD Received 10 Mar 2011; revised 6 Apr 2011; accepted 6 Apr 2011; published 18 Apr 2011

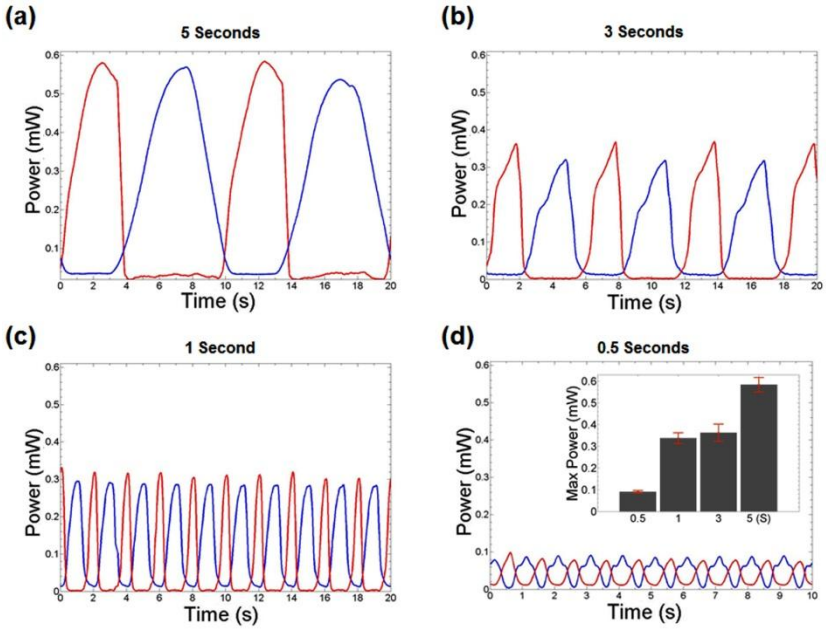

Fig. 5. Output power *vs.* switching period for (a) 5 seconds, (b) 3 seconds, (c) 1 second, and (d) 0.5 seconds. (Inset) Maximum power plot for each switching period. The error bars represents standard error of mean.

Figure 5 shows the relationship between the measured output power and the switching period. The two output channels are represented by blue and red lines. As expected, when the switching period is decreased from 5 seconds to 0.5 seconds, the maximum output power is also decreased from 0.584 mW to 0.0907 mW. The maximum coupled power for all switching periods is plotted in the inset of Fig. 5(d). For these experiments, cross-talk is defined as the ratio of the power coupled into the on fiber to that coupled into the off fiber. Without carbon black doping of the PDMS, the cross-talk was on the order of 10 dB. Introducing carbon black into the chip served to absorb the vast majority of the truant scattered light in the system, reducing the cross-talk down to the 20 dB levels shown in Fig. 5. As can be seen, the quality of the switching also decreased for quicker switching periods placing an upper limit on the rate at which this technique could be used to reconfigure a photonic system. Higher performance may be able to be obtained either by introducing immiscible fluids or using pneumatically actuated PDMS membrane microvalves as has been demonstrated previously [27]. Commercially available MEMS (Microelectromechanical systems) or prism based optical switching devices have shown lower cross-talk (50-80 dB) and faster switching (milliseconds) however the optofluidic switch has advantages including: low insertion coupling loss (3.1 dB) and potential cost advantages as mentioned above.

3.3. Bandwidth

To characterize the optical bandwidth of the system the attenuated power *vs.* core width experiments described above were repeated for four different lasers with wavelengths of 405 nm, 488 nm, 1064 nm, and 1550 nm. All experiments were done using a 1.25 mm liquid waveguide as it showed the maximum transmitted power in the earlier experiments (see Fig. 3(b)). Since each test laser had a different input power value, the output power of the chip was normalized against the input power to the chip from the waveguide. As illustrated in Fig. 6(a), the output power for all wavelengths showed a linear response to waveguide width for both visible and telecommunication wavelengths. Figure 6(b) shows the maximum output power as a function of wavelength. These results show a peak at the blue end of the visible

#143705 - $15.00 USD Received 10 Mar 2011; revised 6 Apr 2011; accepted 6 Apr 2011; published 18 Apr 2011

spectrum and match well with the water absorption spectrum suggesting that this is the limiting factor in the bandwidth of our system. Higher performance can be obtained by using waveguiding fluids whose absorption spectrum are better matched to the wavelength range of interest. For example, at 1550 nm, heavy water would be preferable as a waveguiding fluid for lower optical absorption [30].

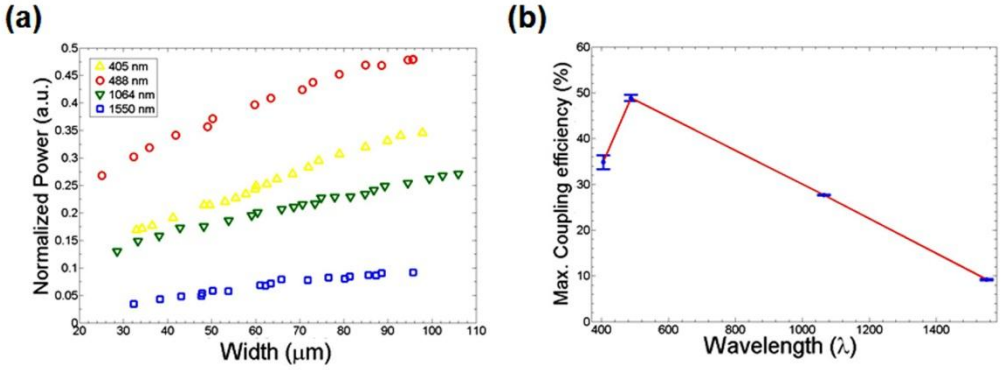

Fig. 6. (a) Coupled power into the output waveguide as a function of core width for 4 different slaser wavelengths. (b) Maximum coupling efficiency for all wavelengths tested here. The error bars represents standard error of the mean.

4. Conclusions

We present here a new approach to reconfigurable photonics which couples the physical adaptability of microfluidic waveguides to fiber-in and fiber-out optical systems. Our efforts focused on the development of two components that could form the basis of a more complex reconfigurable photonic system: a signal attenuator and a 1x2 optical switch. By integrating liquid- and solid-state photonic modalities onto a single chip, we have demonstrated high coupling efficiency (3.1 dB), low cross-talk (less than 20 dB), and demonstrated good performance over a broad range of wavelengths from visible and telecommunication.

Acknowledgments

The authors would like to thank Y-F. Chen for his contribution to the LabVIEW program used to run the experiments, and E. Jung and B. Romero for helpful discussion. The facilities used for this research include the Nanoscale Science & Technology Facility (CNF) and the Nanobiotechnology Center (NBTC) at Cornell University. This work was supported by the Air Force Office of Scientific Research through an STTR grant under the Reconfigurable Materials for Cellular Electronic and Photonic Systems discovery challenge thrust.

#143705 - $15.00 USD Received 10 Mar 2011; revised 6 Apr 2011; accepted 6 Apr 2011; published 18 Apr 2011